INSTITUTE OF MATHEMATICS

THE CZECH ACADEMY OF SCIENCES

Computational comparison of methods for two-sided bounds of eigenvalues

Tomáš Vejchodský

Preprint No. 9-2016

PRAHA 2016

Computational comparison of methods for two-sided bounds of eigenvalues

Tomáš Vejchodský*
Institute of Mathematics, Czech Academy of Sciences,
Žitná 25, Praha 1, CZ-115 67, Czech Republic,
e-mail: vejchod@math.cas.cz

February 29, 2016

Abstract

We compare three finite element based methods for two-sided bounds of eigenvalues of symmetric elliptic operators. The first method is known as eigenvalue inclusions and it is described in [6]. The second method is based on Crouzeix–Raviart nonconforming finite element method [11] and the third one is a combination of the *a priori-a posteriori* inequalities with complementarity based estimators [25]. We briefly describe all three methods and use them to solve two numerical examples. We compare their accuracy, computational performance, and generality.

Keywords: lower bound; spectrum; finite element method; guaranteed bounds; a priori-a posteriori inequalitites; eigenvalue inclusions; Crouzeix–Raviart elements
MSC 2010: 65N25, 65N30

1 Introduction

The standard conforming finite element discretization of symmetric elliptic eigenvalue problems [3, 7] is very efficient and since it is a special case of the Ritz-Galerkin method, it yields natural upper bounds on the exact eigenvalues. Interestingly, lower bounds are much more difficult to compute. The problem of lower bounds attracts attention for many decades. The lower bound of Temple [26] from 1928 was generalized by Kato [18] in 1949 and subsequently by Harrell [12]. Further lower bounds are due to Lehmann [20, 21]. More recently a method of eigenvalue inclusions was developed, see [5] and the overview in [23]. These lower bounds are, however, formulated in an abstract way using linear operators on Hilbert spaces and it is not straightforward to use these results in

*The author gratefully acknowledges the institutional support RVO 67985840.

the context of the finite element method. A practical approach how to compute the eigenvalue inclusions by the finite element method is described in [6] and we use this approach below as the first method for the comparison.

In 2013 Carstensen and Gedicke [11] published a lower bound based on Crouzeix–Raviart finite elements. We choose this method as the second one for the comparison. Let us note that there exist several methods for lower bounds on eigenvalues based on nonconforming finite elements, see e.g. [2, 22, 1, 16, 17, 30]. However, the distinctive feature of the chosen method is that it does not require an *a priori* information about the spectrum and provides guaranteed lower bounds even on rough meshes. The third method, we present and compare is based on a combination of *a priori-a posteriori* inequalities [19] with complementarity based estimators, see [25, 24].

Generality of the chosen methods varies. The method based on Crouzeix–Raviart elements is the least general, because it is designed specifically for the Laplace eigenvalue problem with homogeneous Dirichlet boundary conditions. This is also the reason, why we choose this type of problem for the comparison. We seek eigenvalues λ_i and eigenfunctions $u_i \neq 0$, $i = 1, 2, \ldots$, defined in an open domain $\Omega \subset \mathbb{R}^2$ such that

$$\begin{aligned} -\Delta u_i &= \lambda_i u_i \quad \text{in } \Omega, \\ u_i &= 0 \qquad \text{on } \partial\Omega. \end{aligned} \tag{1}$$

The weak formulation of this problem is based on the Sobolev space $V = H_0^1(\Omega)$ of square integrable functions with square integrable distributional derivatives and zero traces on the boundary $\partial\Omega$. Note that due to the well posedness, we assume Ω to be Lipschitz domain. Denoting the $L^2(\Omega)$ inner product by $(\cdot, \cdot)$, the weak formulation reads: find $\lambda_i \in \mathbb{R}$ and $u_i \in V$, $u_i \neq 0$, such that

$$(\nabla u_i, \nabla v) = \lambda_i (u_i, v) \quad \forall v \in V. \tag{2}$$

It is well known [3, 7] that the eigenvalues λ_i are positive, tend to infinity, and form a countable sequence. We consider the natural enumeration $0 < \lambda_1 \leq \lambda_2 \leq \cdots$ and repeat the eigenvalues according to their multiplicity. Our goal is to use the three chosen methods and compute the lower and the upper bound for the first m eigenvalues.

The subsequent Sections 2–4 describe the three methods we compare. Section 5 presents the numerical performance of the three methods on a square domain, where the analytic solution is known. Section 6 provides the results for a dumbbell shaped domain, where the analytic solution is not available. Finally, Section 7 draws the conclusions.

2 The method of eigenvalue inclusions

In this section, we describe the method from [6] and we will refer to it as the inclusions method. The upper bound on eigenvalues is obtained by the standard conforming finite element method. For simplicity we consider Ω to be a polygon.

We denote the standard finite element triangulation of Ω by $\mathcal{T}_h$, and define the lowest-order finite element space

$$V_h = \{v_h \in V : v_h|_K \in P_1(K) \quad \forall K \in \mathcal{T}_h\}, \tag{3}$$

where $P_1(K)$ is the space of affine functions on the triangle K. The finite element approximation of problem (1) consists of seeking eigenvalues $\Lambda_{h,i} \in \mathbb{R}$ and eigenfunctions $u_{h,i} \in V_h$ such that

$$(\nabla u_{h,i}, \nabla v_h) = \Lambda_{h,i}(u_{h,i}, v_h) \quad \forall v_h \in V_h. \tag{4}$$

It is well known that the approximate eigenvalues $\Lambda_{h,i}$ provide upper bounds on the exact eigenvalues: $\lambda_i \le \Lambda_{h,i}$ for all $i = 1, 2, \ldots$.

The lower bounds on eigenvalues are based on the result provided in [6, Theorem 2.1]. For the readers' convenience, we present this result here as Theorem 1. Note that $\boldsymbol{W} = \boldsymbol{H}(\mathrm{div}, \Omega)$ denotes the space of square integrable vector fields with square integrable divergence.

Theorem 1. *Let $(\tilde{u}_i, \tilde{\boldsymbol{\sigma}}_i) \in V \times \boldsymbol{W}$, $i = 1, 2, \ldots, n$, and $\rho > 0$, $\gamma > 0$ be arbitrary. Define matrices $\boldsymbol{M}, \boldsymbol{N} \in \mathbb{R}^{n\times n}$ with entries*

$$\boldsymbol{M}_{ij} = (\nabla \tilde{u}_i, \nabla \tilde{u}_j) + (\gamma - \rho)(\tilde{u}_i, \tilde{u}_j),$$
$$\boldsymbol{N}_{ij} = (\nabla \tilde{u}_i, \nabla \tilde{u}_j) + (\gamma - 2\rho)(\tilde{u}_i, \tilde{u}_j) + \rho^2(\tilde{\boldsymbol{\sigma}}_i, \tilde{\boldsymbol{\sigma}}_j) + (\rho^2/\gamma)(\tilde{u}_i + \mathrm{div}\, \tilde{\boldsymbol{\sigma}}_i, \tilde{u}_j + \mathrm{div}\, \tilde{\boldsymbol{\sigma}}_j).$$

Suppose, that the matrix $\boldsymbol{N}$ is positive definite, and let

$$\mu_1 \le \mu_2 \le \cdots \le \mu_n$$

be the eigenvalues of the generalized eigenvalue problem

$$\boldsymbol{M}\boldsymbol{y}_i = \mu_i \boldsymbol{N}\boldsymbol{y}_i, \quad i = 1, 2, \ldots, n.$$

Then, for all i such that $\mu_i < 0$, the interval

$$[\rho - \gamma - \rho/(1 - \mu_i), \rho - \gamma)$$

contains at least i eigenvalues of the continuous problem (2).

Functions $\tilde{u}_i \in V$ and $\tilde{\boldsymbol{\sigma}}_i \in \boldsymbol{W}$ in Theorem 1 are in general arbitrary, but in order to obtain accurate bounds, they should approximate the exact eigenfunction u_i and the corresponding flux $\lambda_i^{-1}\nabla u_i$, respectively. The natural choice for $\tilde{u}_i$ is the finite element approximation $u_{h,i}$. The choice of $\tilde{\boldsymbol{\sigma}}_i$ is based on the complementarity technique [28, 29], also known as the dual finite elements [13, 14, 15]. It is proposed in [6] to set $\tilde{\boldsymbol{\sigma}}_i = \boldsymbol{\sigma}_{h,i}$, where $\boldsymbol{\sigma}_{h,i}$ is a solution of a saddle point problem solved by the mixed finite element method. We denote by $P_k(K)$ the space of polynomials of degree at most k on the triangle $K \in \mathcal{T}_h$ and by

$$\mathbf{RT}_k(K) = [P_k(K)]^2 \oplus \boldsymbol{x}P_k(K) \tag{5}$$

the Raviart–Thomas space on the element $K \in \mathcal{T}_h$. The flux reconstruction $\boldsymbol{\sigma}_{h,i}$ is sought in the Raviart–Thomas space

$$\boldsymbol{W}_h = \{\boldsymbol{\sigma}_h \in \boldsymbol{H}(\mathrm{div}, \Omega) : \boldsymbol{\sigma}_h|_K \in \mathbf{RT}_k(K) \quad \forall K \in \mathcal{T}_h\},$$

and the Lagrange multipliers in

$$Q_h = \{q_h \in L^2(\Omega) : q_h|_K \in P_k(K) \quad \forall K \in \mathcal{T}_h\}.$$

The mixed finite element problem then reads: find $(\boldsymbol{\sigma}_{h,i}, q_{h,i}) \in \boldsymbol{W}_h \times Q_h$ such that

$$(\boldsymbol{\sigma}_{h,i}, \boldsymbol{w}_h) + (q_{h,i}, \mathrm{div}\, \boldsymbol{w}_h) = 0 \qquad \forall \boldsymbol{w}_h \in \boldsymbol{W}_h, \tag{6}$$

$$(\mathrm{div}\, \boldsymbol{\sigma}_{h,i}, \varphi) = (-u_{h,i}, \varphi) \quad \forall \varphi \in Q_h, \tag{7}$$

where $u_{h,i} \in V_h$ is the finite element approximation (4).

Paper [6] proposes to choose $k = 0$ for linear finite elements, see (3). However, this choice seems to be suboptimal and we observed slow speed of convergence in test examples. Therefore, we choose $k = 1$ in what follows.

To obtain lower bounds on eigenvalues based on Theorem 1, we need an *a priori* information about the eigenvalues. Namely, if $\rho - \gamma \le \lambda_L$ for some index $L \ge 2$ then Theorem 1 provides lower bounds

$$\rho - \gamma - \rho/(1 - \mu_i) \le \lambda_{L-i} \quad \forall i = 1, 2, \ldots, \min\{L - 1, n\}. \tag{8}$$

Thus, if we know an *a priori* lower bound on at least one exact eigenvalue then we can compute lower bounds on eigenvalues below this one by (8).

In the numerical examples below, we use rough lower bounds $\underline{\lambda}_i$, $i = 1, 2, \ldots, m+1$ for the first $m+1$ eigenvalues. Utilizing this information, we compute accurate lower bounds on the first m eigenvalues as follows.

1. We compute the standard finite element approximations (4) of the first m eigenpairs $(\Lambda_{h,i}, u_{h,i}) \in \mathbb{R} \times V_h$, $i = 1, 2, \ldots, m$. This provides upper bounds $\Lambda_{h,i}$, $i = 1, 2, \ldots, m$, on the exact eigenvalues.

2. We find $\boldsymbol{\sigma}_{h,i} \in \boldsymbol{W}_h$ by solving (6)–(7).

3. For all $n = 1, 2, \ldots, m$, we apply Theorem 1 with $\tilde{u}_i = u_{h,i}$, $\tilde{\boldsymbol{\sigma}}_i = \boldsymbol{\sigma}_{h,i}$, $i = 1, 2, \ldots, n$, $\gamma^{(n)} = \|u_{h,n} + \mathrm{div}\, \boldsymbol{\sigma}_{h,n}\|_{L^2(\Omega)}$ and $\rho^{(n)} = \underline{\lambda}_{n+1} + \gamma$. We assemble matrices $\boldsymbol{M}^{(n)}$ and $\boldsymbol{N}^{(n)}$ and find the eigenvalues $\mu_1^{(n)} \le \mu_2^{(n)} \le \cdots \le \mu_n^{(n)}$. The assumptions of the positive definiteness of $\boldsymbol{N}^{(n)}$ and of the negativity of $\mu_i^{(n)}$, are easy to check and if they are satisfied then we obtain the lower bound (8). In particular, we choose $L = n + 1$ and $i = n + 1 - j$ in (8) and get

$$\ell_{j,n}^{\mathrm{incl}} = \rho - \gamma - \rho/\left(1 - \mu_{n+1-j}^{(n)}\right) \le \lambda_j, \quad j = 1, 2, \ldots, n.$$

As the final lower bound, we take the largest of these values, namely

$$\ell_j^{\mathrm{incl}} = \max\{\ell_{j,n}^{\mathrm{incl}},\ n = j, j+1, \ldots, m\}, \quad j = 1, 2, \ldots, m.$$

Note that here we provide the description of the method of eigenvalue inclusions tailored to the test problem (1). In [6], the method is described for the Laplace eigenvalue problem with mixed homogeneous Dirichlet and Neumann boundary conditions. However, it is clearly not limited to such simple problems and can be straightforwardly generalized to problems with reaction terms and with variable diffusion and reaction coefficient.

3 The method based on Crouzeix–Raviart elements

In this section, we describe the method from [11] and we will refer to it as the CR method, because it is based on Crouzeix–Raviart finite elements. We consider the triangulation $\mathcal{T}_h$ of Ω as above. Further, we define the space of piecewise affine and in general discontinuous functions as

$$\mathcal{P}_1(\mathcal{T}_h) = \{v_h \in L^2(\Omega) : v_h|_K \in P_1(K)\}.$$

We also denote by $\mathcal{E}_h$ the set of all edges in $\mathcal{T}_h$ and define the standard Crouzeix–Raviart finite element space as

$$V_h^{\mathrm{CR}} = \{v_h \in \mathcal{P}_1(\mathcal{T}_h) : v_h \text{ is continuous in the midpoint of each edge } \gamma \in \mathcal{E}_h\}.$$

The Crouzeix–Raviart approximate eigenpairs $(\lambda_{h,i}^{\mathrm{CR}}, u_{h,i}^{\mathrm{CR}}) \in \mathbb{R}\times V_h^{\mathrm{CR}}$, $u_{h,i}^{\mathrm{CR}} \neq 0$, of problem (1) are defined by the relation

$$(\nabla u_{h,i}^{\mathrm{CR}}, \nabla v_h) = \lambda_{h,i}^{\mathrm{CR}}(u_{h,i}^{\mathrm{CR}}, v_h) \quad \forall v_h \in V_h^{\mathrm{CR}}. \tag{9}$$

The approximate eigenvalues $\lambda_{h,i}^{\mathrm{CR}}$ are often below the exact eigenvalues λ_i, but not always. Especially on very rough meshes it is not difficult to construct an example such that $\lambda_{h,i}^{\mathrm{CR}}$ is above λ_i, see [11]. However, explicit estimates of the interpolation constant enable to construct simple lower bounds on exact eigenvalues. It is proved in [11, Theorem 3.2 and 5.1] that

$$\ell_i^{\mathrm{CR}} \leq \lambda_i \quad \text{for} \quad \ell_i^{\mathrm{CR}} = \frac{\lambda_{h,i}^{\mathrm{CR}}}{1 + \kappa^2 \lambda_{h,i}^{\mathrm{CR}} h_{\max}^2}, \quad \forall i = 1, 2, \ldots, \tag{10}$$

where $\kappa^2 = 1/8 + j_{1,1}^{-2}$, symbol $j_{1,1}$ stands for the first positive root of the Bessel function of the first kind, and $h_{\max} = \max_{K\in\mathcal{T}_h} \operatorname{diam} K$ is the largest of all diameters of elements in the triangulation $\mathcal{T}_h$. Note that κ^2 is a universal constant and we use the bound $\kappa^2 \leq 0.1932$ in the subsequent numerical examples to compute the guaranteed lower bounds.

Let us note that problem (9) is equivalent to the matrix eigenvalue problem

$$\boldsymbol{A}\boldsymbol{u}_i^{\mathrm{CR}} = \lambda_{h,i}^{\mathrm{CR}} \boldsymbol{B}\boldsymbol{u}_i^{\mathrm{CR}}, \tag{11}$$

where matrices $\boldsymbol{A}, \boldsymbol{B} \in \mathbb{R}^{N^{\mathrm{CR}}\times N^{\mathrm{CR}}}$ have entries $\boldsymbol{A}_{jk} = (\nabla\varphi_j, \nabla\varphi_k)$ and $\boldsymbol{B}_{jk} = (\varphi_j, \varphi_k)$, functions φ_j, $j = 1, 2, \ldots, N^{\mathrm{CR}}$, are the standard edge-based Crouzeix–Raviart basis functions in V_h^{CR}, and $N^{\mathrm{CR}} = \dim V_h^{\mathrm{CR}}$. The entries of the vector

$\boldsymbol{u}_i^{\mathrm{CR}}$ are then coefficients in the expansion of the approximate eigenfunction $u_{h,i}^{\mathrm{CR}}$ in this basis, i.e. $u_{h,i}^{\mathrm{CR}} = \sum_{j=1}^{N^{\mathrm{CR}}} \left(\boldsymbol{u}_i^{\mathrm{CR}}\right)_j \varphi_j$. The point is that the lower bound (10) is valid only if $\lambda_{h,i}^{\mathrm{CR}}$ and $u_{h,i}^{\mathrm{CR}}$ satisfy equality (9) *exactly*. This is however never the case in practice, because the round-off and iteration errors prevent us to solve the matrix eigenvalue problem (11) exactly. Nevertheless, the approach presented in [11] solves this problem as well.

If $(\tilde{\lambda}_{h,i}^{\mathrm{CR}}, \tilde{u}_{h,i}^{\mathrm{CR}}) \in \mathbb{R} \times V_h^{\mathrm{CR}}$ is an arbitrary approximation of the exact eigenpair and if $\boldsymbol{r} = \boldsymbol{A}\tilde{\boldsymbol{u}}_i^{\mathrm{CR}} - \tilde{\lambda}_{h,i}^{\mathrm{CR}} \boldsymbol{B}\tilde{\boldsymbol{u}}_i^{\mathrm{CR}}$ with $\tilde{u}_{h,i}^{\mathrm{CR}} = \sum_{j=1}^{N^{\mathrm{CR}}} \left(\tilde{\boldsymbol{u}}_i^{\mathrm{CR}}\right)_j \varphi_j$ is the corresponding algebraic residual then [11, Theorems 3.1 and 5.1] provide lower bounds

$$\tilde{\ell}_i^{\mathrm{CR}} \le \lambda_i \quad \text{for} \quad \tilde{\ell}_i^{\mathrm{CR}} = \frac{\lambda_{h,i}^{\mathrm{CR}} - \|\boldsymbol{r}\|_{\boldsymbol{B}^{-1}}}{1 + \kappa^2 \left(\lambda_{h,i}^{\mathrm{CR}} - \|\boldsymbol{r}\|_{\boldsymbol{B}^{-1}}\right) h_{\max}^2}, \quad \forall i = 1, 2, \ldots, \tag{12}$$

where $\|\boldsymbol{r}\|_{\boldsymbol{B}^{-1}}^2 = \boldsymbol{r}^\top \boldsymbol{B}^{-1} \boldsymbol{r}$. The lower bound (12) is valid if $\|\boldsymbol{r}\|_{\boldsymbol{B}^{-1}} < \tilde{\lambda}_{h,i}^{\mathrm{CR}}$ and if $\tilde{\lambda}_{h,i}^{\mathrm{CR}}$ is closer to the exact discrete eigenvalue $\lambda_{h,i}^{\mathrm{CR}}$ than to any other discrete eigenvalue $\lambda_{h,j}^{\mathrm{CR}}$, $j \neq i$. This closeness assumption is difficult to verify, because the exact discrete eigenvalues are not know. If the eigenvalues are tightly clustered then this assumption can be violated even if the residual $\boldsymbol{r}$ is relatively small. Note that in the numerical examples below, we have $\|\boldsymbol{r}\|_{\boldsymbol{B}^{-1}}$ always below 10^{-10} and hence the correction (12) has virtually no effect in comparison with (10).

Concerning the upper bound on eigenvalues, we can well use the standard conforming finite element approximations given by (4). This would, however, mean to solve one more matrix eigenvalue problem. Therefore the authors of [11] propose to use a conforming interpolation of the already computed nonconforming eigenfunction $\tilde{u}_{h,i}^{\mathrm{CR}}$. They use the interpolation operator $\mathcal{I}_{\mathrm{CM}} : V_h^{\mathrm{CR}} \to V_h^*$, where $V_h^* = \{v_h \in V : v_h|_K \in P_1(K)\ \forall K \in \mathcal{T}_h^*\}$ and $\mathcal{T}_h^*$ is the uniform (red) refinement of the triangulation $\mathcal{T}_h$ such that all triangles in $\mathcal{T}_h$ are refined into four similar subtriangles of $\mathcal{T}_h^*$. The interpolation $\mathcal{I}_{\mathrm{CM}}$ was proposed in [10], see also [11]. If $\mathcal{N}_h$ stands for the set of all vertices of the triangulation $\mathcal{T}_h$ and $\mathcal{E}_h$ for the set of all edges in $\mathcal{T}_h$ and if $v_h^{\mathrm{CR}} \in V_h^{\mathrm{CR}}$ is arbitrary then

$$\left(\mathcal{I}_{\mathrm{CM}} v_h^{\mathrm{CR}}\right)(\boldsymbol{z}) = \begin{cases} 0 & \text{if } \boldsymbol{z} \text{ lies on } \partial\Omega, \\ v_h^{\mathrm{CR}}(\boldsymbol{z}) & \text{if } \boldsymbol{z} \text{ is the midpoint of an edge } \gamma \in \mathcal{E}_h,\ \gamma \not\subset \partial\Omega, \\ v_{\min}(\boldsymbol{z}) & \text{if } \boldsymbol{z} \in \mathcal{N}_h \setminus \partial\Omega. \end{cases}$$

The function $v_{\min}$ is determined by a one-dimensional minimization on the patch $\omega_{\boldsymbol{z}}^*$ of elements from $\mathcal{T}_h^*$ sharing the vertex $\boldsymbol{z}$. We set $V_{\boldsymbol{z}} = \{v_h \in C(\overline{\omega}_{\boldsymbol{z}}^*) : v_h|_K \in P_1(K)$ for all $K \in \mathcal{T}_h^*,\ K \subset \overline{\omega}_{\boldsymbol{z}}^*$, and $v_h = v_h^{\mathrm{CR}}$ on $\partial\omega_{\boldsymbol{z}}^*\}$ and determine $v_{\min} \in V_{\boldsymbol{z}}$ as the unique minimizer of

$$\min_{v_h \in V_{\boldsymbol{z}}} \left\| \nabla v_h^{\mathrm{CR}} - \nabla v_h \right\|_{L^2(\omega_{\boldsymbol{z}}^*)}.$$

Then, the Rayleigh quotients constructed from $u_{h,i}^* = \mathcal{I}_{\mathrm{CM}} \tilde{u}_{h,i}^{\mathrm{CR}}$ provide the upper bounds in a standard way.

In particular, since our goal is to obtain lower and upper bounds for the first m eigenvalues, we proceed as follows.

1. We solve the Crouzeix–Raviart eigenvalue problem (9) for $i = 1, 2, \ldots, m$. The resulting eigenpairs polluted by the round-off and iteration errors are denoted by $\tilde{\lambda}_{h,i}^{\mathrm{CR}}$ and $\tilde{u}_{h,i}^{\mathrm{CR}}$.

2. We use these approximations and compute lower bounds $\tilde{\ell}_i^{\mathrm{CR}}$ by (12) for $i = 1, 2, \ldots, m$.

3. We construct the uniform (red) refinement $\mathcal{T}_h^*$ of the mesh $\mathcal{T}_h$ and interpolants $u_{h,i}^* = \mathcal{I}_{\mathrm{CM}} \tilde{u}_{h,i}^{\mathrm{CR}}$ for $i = 1, 2, \ldots, m$.

4. Using the standard Ritz-Galerkin method, we assemble matrices $\boldsymbol{S}, \boldsymbol{Q} \in \mathbb{R}^{m \times m}$ with entries $\boldsymbol{S}_{j,k} = (\nabla u_{h,j}^*, \nabla u_{h,k}^*)$ and $\boldsymbol{Q}_{j,k} = (u_{h,j}^*, u_{h,k}^*)$ and solve the matrix eigenvalue problem

$$\boldsymbol{S}\boldsymbol{y}_i = \Lambda_i^* \boldsymbol{Q}\boldsymbol{y}_i, \quad i = 1, 2, \ldots, m.$$

   We sort these eigenvalues such that $\Lambda_1^* \leq \Lambda_2^* \leq \cdots \leq \Lambda_m^*$ and we have the upper bounds

$$\lambda_i \leq \Lambda_i^* \quad \text{for } i = 1, 2, \ldots, m.$$

4 The complementarity method

In this section, we describe the method introduced in [25] and we will refer to it as the complementarity method. It is based on the standard conforming finite element approximation (4). Lower bounds on eigenvalues are obtained by the method of *a priori-a posteriori* inequalities [19] using the complementarity technique and local flux reconstruction [8].

We consider the triangulation $\mathcal{T}_h$ of the domain Ω as above and the finite element approximate eigenpair $(\Lambda_{h,i}, u_{h,i}) \in \mathbb{R} \times V_h$ as in (4). Based on the gradient $\nabla u_{h,i}$ of the approximate eigenvector, we construct a suitable flux $\boldsymbol{q}_{h,i} \in \boldsymbol{H}(\mathrm{div}, \Omega)$. This flux is constructed by solving small mixed finite element problems on patches of elements sharing a single vertex. Let $\boldsymbol{z} \in \mathcal{N}_h$ be a vertex in $\mathcal{T}_h$ and let $\mathcal{T}_{\boldsymbol{z}}$ be the set of those elements in $\mathcal{T}_h$ that $\boldsymbol{z}$ is one of their vertices. By $\omega_{\boldsymbol{z}} = \mathrm{int} \bigcup \{K : K \in \mathcal{T}_{\boldsymbol{z}}\}$ we denote the patch of elements sharing the vertex $\boldsymbol{z}$. If $\boldsymbol{z}$ is an interior vertex then we set $\Gamma_{\omega_{\boldsymbol{z}}}^{\mathrm{ext}} = \partial\omega_{\boldsymbol{z}}$ and if $\boldsymbol{z}$ lies on the boundary $\partial\Omega$ then we set $\Gamma_{\omega_{\boldsymbol{z}}}^{\mathrm{ext}} = \partial\omega_{\boldsymbol{z}} \setminus \partial\Omega$. We denote by $\boldsymbol{n}_{\omega_{\boldsymbol{z}}}$ the unit outward facing normal vector to $\partial\omega_{\boldsymbol{z}}$ and define spaces

$$\boldsymbol{W}_{\boldsymbol{z}} = \left\{ \boldsymbol{w}_h \in \boldsymbol{H}(\mathrm{div}, \omega_{\boldsymbol{z}}) : \boldsymbol{w}_h|_K \in \mathbf{RT}_1(K) \ \forall K \in \mathcal{T}_{\boldsymbol{z}} \quad \text{and} \quad \boldsymbol{w}_h \cdot \boldsymbol{n}_{\omega_{\boldsymbol{z}}} = 0 \text{ on } \Gamma_{\omega_{\boldsymbol{z}}}^{\mathrm{ext}} \right\}$$

and

$$\mathcal{P}_1^*(\mathcal{T}_{\boldsymbol{z}}) = \begin{cases} \{v_h \in \mathcal{P}_1(\mathcal{T}_{\boldsymbol{z}}) : \int_{\omega_{\boldsymbol{z}}} v_h \,\mathrm{d}x = 0\} & \text{for interior vertices } \boldsymbol{z} \in \mathcal{N}_h \setminus \partial\Omega, \\ \mathcal{P}_1(\mathcal{T}_{\boldsymbol{z}}) & \text{for boundary vertices } \boldsymbol{z} \in \mathcal{N}_h \cap \partial\Omega. \end{cases}$$

We recall that spaces $\mathbf{RT}_k(K)$ were introduced in (5) and $\mathcal{P}_1(\mathcal{T}_{\boldsymbol{z}})$ stands for the space of piecewise affine and in general discontinuous functions. Further, we denote by $\psi_{\boldsymbol{z}}$ the standard piecewise affine and continuous finite element hat function associated with the vertex $\boldsymbol{z} \in \mathcal{N}_h$. Function $\psi_{\boldsymbol{z}}$ has value one at $\boldsymbol{z}$ and vanishes at all other vertices of the triangulation $\mathcal{T}_h$. We also introduce the residual

$$r_{\boldsymbol{z},i} = \Lambda_{h,i}\psi_{\boldsymbol{z}}u_{h,i} - \nabla\psi_{\boldsymbol{z}} \cdot \nabla u_{h,i}.$$

The flux reconstruction $\boldsymbol{q}_{h,i} \in \boldsymbol{H}(\mathrm{div}, \Omega)$ is then defined as

$$\boldsymbol{q}_{h,i} = \sum_{\boldsymbol{z}\in\mathcal{N}_h} \boldsymbol{q}_{\boldsymbol{z},i}, \tag{13}$$

where $\boldsymbol{q}_{\boldsymbol{z},i} \in \boldsymbol{W}_{\boldsymbol{z}}$ together with $d_{\boldsymbol{z},i} \in \mathcal{P}_1^*(\mathcal{T}_{\boldsymbol{z}})$ solves the mixed finite element problem

$$(\boldsymbol{q}_{\boldsymbol{z},i}, \boldsymbol{w}_h)_{\omega_{\boldsymbol{z}}} - (d_{\boldsymbol{z},i}, \mathrm{div}\, \boldsymbol{w}_h)_{\omega_{\boldsymbol{z}}} = (\psi_{\boldsymbol{z}}\nabla u_{h,i}, \boldsymbol{w}_h)_{\omega_{\boldsymbol{z}}} \quad \forall \boldsymbol{w}_h \in \boldsymbol{W}_{\boldsymbol{z}}, \tag{14}$$

$$-(\mathrm{div}\, \boldsymbol{q}_{\boldsymbol{z},i}, \varphi_h)_{\omega_{\boldsymbol{z}}} = (r_{\boldsymbol{z},i}, \varphi_h)_{\omega_{\boldsymbol{z}}} \quad \forall \varphi_h \in \mathcal{P}_1^*(\mathcal{T}_{\boldsymbol{z}}). \tag{15}$$

The reconstructed flux $\boldsymbol{q}_{h,i}$ is used to define the error estimator

$$\eta_i = \left\| \nabla u_{h,i} - \boldsymbol{q}_{h,i} \right\|_{L^2(\Omega)}.$$

This is further used to define the lower bound on the lowest eigenvalue

$$\ell_1^{\mathrm{cmpl}} = \left(-\eta_1 + \sqrt{\eta_1^2 + 4\Lambda_{h,1}} \right)^2 /4 \tag{16}$$

and the lower bound on the higher eigenvalues

$$\ell_i^{\mathrm{cmpl}} = \Lambda_{h,i} \left(1 + \underline{\lambda}_1^{-1/2}\eta_i \right)^{-1}, \quad i = 2, 3, \ldots, \tag{17}$$

where $\underline{\lambda}_1$ is a lower bound on λ_1. It is natural to choose $\underline{\lambda}_1 = \ell_1^{\mathrm{cmpl}}$, but due to consistency with the inclusion method, we will use in the subsequent numerical examples an *a priori* known rough lower bound $\underline{\lambda}_1$ on the first eigenvalue.

For a given $i = 1, 2, \ldots$, the lower bound ℓ_i^{cmpl} is proved in [25] to be below the exact eigenvalue λ_i if the relative closeness assumption

$$\Lambda_{h,i} \leq 2 \left(\lambda_i^{-1} + \lambda_{i+1}^{-1} \right)^{-1} \tag{18}$$

is satisfied. This assumption is difficult to verify unless lower bounds on the exact eigenvalues are known. Similarly, as in the case of the inclusion method, the validity of the relative closeness assumption is an *a priori* information needed to guarantee that the computed bounds are really below the exact eigenvalues. However, this *a priori* information is of a different nature than the *a priori* information in the inclusion method. The relative closeness assumption requires the standard finite element approximation $\Lambda_{h,i}$ to be sufficiently close to the

	a priori lower bound	the largest lower bound	exact eigenvalue	the smallest upper bound
λ_1	1.652893	1.999982	2	2.000006
λ_2	4.132231	4.999429	5	5.000034
λ_3	4.132231	4.999549	5	5.000034
λ_4	6.611570	7.997871	8	8.000100
λ_5	8.264463	9.996874	10	10.000162
λ_6	8.264463	9.996874	10	10.000162
λ_7	10.743802	12.994457	13	13.000281
λ_8	10.743802	12.994457	13	13.000281
λ_9	14.049587	16.991093	17	17.000457
λ_{10}	14.049587	16.991093	17	17.000457

Table 1: The analytical *a priori* lower bounds, the largest computed lower bounds, the exact values, and the smallest computed upper bounds of the first 10 eigenvalues for the square domain.

exact eigenvalue λ_i. The sufficient accuracy depends on the size of the spectral gap $\lambda_{i+1} - \lambda_i$. In contrast, the inclusion method requires a guaranteed lower bound on at least one eigenvalue.

To summarize, we apply the complementary method as follows.

1. We compute the standard finite element approximations $(\Lambda_{h,i}, u_{h,i}) \in \mathbb{R} \times V_h$, $i = 1, 2, \ldots, m$, of the first m eigenpairs according to (4). This provides upper bounds $\Lambda_{h,i}$, $i = 1, 2, \ldots, m$, on the exact eigenvalues.

2. For all $i = 1, 2, \ldots, m$ and all vertices $\boldsymbol{z} \in \mathcal{N}_h$, we solve local patch problems (14)–(15) and construct the flux $\boldsymbol{q}_{h,i}$ as in (13).

3. We evaluate lower bounds ℓ_i^{cmpl} using (16) for $i = 1$ and (17) for $i = 2, 3, \ldots, m$.

5 Numerical results – a square domain

In this section we compute two sided bounds of the first $m = 10$ eigenvalues of problem (1) in a square $\Omega = (0, \pi)^2$. We compute these bounds by using the three methods described in Sections 2–4 and compare their numerical performance. In the square domain, the exact eigenvalues and eigenfunctions are well known. They are given by

$$\lambda_{j,k} = j^2 + k^2, \quad u_{j,k}(x, y) = \sin(jx)\sin(ky), \quad j, k = 1, 2, \ldots,$$

and the first 10 exact eigenvalues are listed in the fourth column of Table 1. Notice that four out of the first six distinct eigenvalues are doubled.

As we mentioned in Section 2, for the method of eigenvalue inclusions we require *a priori* known lower bounds on the first $m+1$ eigenvalues. If the exact

eigenvalues for the domain Ω were not known then we can find lower bounds by enclosing Ω into a rectangle $\widehat{\Omega}$ with lengths of sides L_1 and L_2. For this rectangle, we can easily find the eigenvalues analytically:

$$\hat{\lambda}_{j,k} = \pi^2 \left(j^2 L_1^{-2} + k^2 L_2^{-2} \right), \quad j,k = 1,2,\dots.$$

Since $\Omega \subset \widehat{\Omega}$, the eigenvalues on $\widehat{\Omega}$ are smaller than the eigenvalues on Ω.

Due to consistency with the next numerical example, we use this approach for the analytic lower bounds also for the square Ω, although the exact eigenvalues are known. In this particular case, we enclose Ω into a square with side length 1.1π. Consequently, we obtain analytic lower bounds in the form

$$\hat{\lambda}_{j,k} = (10/11)^2 \lambda_{j,k}, \quad j,k = 1,2,\dots.$$

Their approximate numerical values are presented in the second column of Table 1.

For all three methods we use the same triangulations. The initial rough triangulation is shown in Figure 1 (left). Then we obtain a sequence of nested meshes by successive uniform (red) refinement. This means that we refine each triangle of the original mesh into four similar subtriangles.

Given a mesh $\mathcal{T}_h$ of this sequence, we use it for all three methods to compute the lower and upper bound of eigenvalues. The methods, however, use different types of finite elements and consequently, they require to solve matrix problems of different sizes. Therefore, we compare their accuracy with respect to the number of degrees of freedom corresponding to the largest matrix problem that has to be solved. To be more specific, we choose $N^{\mathrm{mix}} = \dim \boldsymbol{W}_h + \dim Q_h$ to be the reference number of degrees of freedom for the inclusions method, because the mixed finite element problem (6)–(7) is considerably larger than problem (4) and its solution consumes most of the computational time. For the CR method, we naturally choose $N^{\mathrm{CR}} = \dim V_h^{\mathrm{CR}}$ as the reference number of degrees of freedom, although the upper bound computed by this method requires the refined mesh $\mathcal{T}_h^*$ and the interpolation $\mathcal{I}_{\mathrm{CM}} \tilde{u}_{h,i}^{\mathrm{CR}}$ with more degrees of freedom then N^{CR}. This interpolation, however, can be done locally on patches and does not consume the majority of the computational time. Finally, for the complementarity method we choose $N^{\mathrm{conf}} = \dim V_h$ as the reference number of degrees of freedom. This method also requires the construction of fluxes $\boldsymbol{q}_{h,i}$ which corresponds to a larger number of degrees of freedom, but again these fluxes can be computed efficiently by solving small local problems on patches.

The most accurate results, i.e. the largest lower bounds and the smallest upper bounds we computed, are provided in Table 1. In Figure 2 we resent the sizes of eigenvalue enclosures, i.e. the differences between the computed upper and lower bound. More precisely the enclosure sizes for the eigenvalue λ_i are given by $\Lambda_{h,i} - \ell_i^{\mathrm{incl}}$ for the inclusions method, by $\Lambda_i^* - \tilde{\ell}_i^{\mathrm{CR}}$ for the CR method, and by $\Lambda_{h,i} - \ell_i^{\mathrm{cmpl}}$ for the complementarity method. Figure 2 shows the convergence of these enclosures as the mesh is uniformly refined and the number

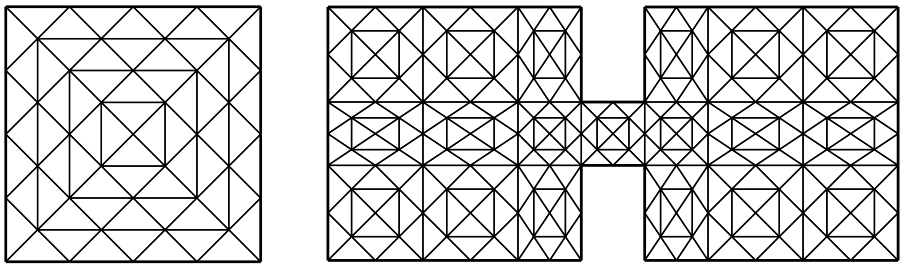

Figure 1: Initial triangulations of the square domain (left) and the dumbbell shaped domain (right).

of degrees of freedom increases. We immediately observe that if N stands for the respective number of degrees of freedom then the enclosures converge as $O(N^{-1})$ for the inclusion and CR methods and as $O(N^{-1/2})$ for the complementarity method, see the experimental orders of convergence indicated in Figure 2. If $h = \max_{K\in\mathcal{T}_h} \operatorname{diam} K$ stands for the standard mesh size parameter then this corresponds to the expected $O(h^2)$ convergence of the inclusion and CR methods and to the suboptimal $O(h)$ convergence of the complementarity method. This suboptimal convergence is caused by the suboptimal rate of convergence of the lower bound ℓ_i^{cmpl}, because the upper bound provided by the standard finite element approximation $\Lambda_{h,i}$ is known to converge quadratically [3, 7].

We also observe that the CR method provides the smallest eigenvalue enclosure with respect to the needed number of degrees of freedom. The inclusion method closely follows for the smaller eigenvalues. However, for larger eigenvalues the inclusion method legs behind and for λ_9 and λ_{10} it even fails to converge and it does not provide an acceptable accuracy of the lower bound. This is caused by too rough *a priori* lower bounds. For the lower bound on λ_1 the method utilizes all *a priori* lower bounds $\underline{\lambda}_2, \ldots, \underline{\lambda}_{11}$ and combining all this information yields accurate bounds. However, for λ_{10} we can use only the *a priori* lower bound $\underline{\lambda}_{11}$, which is so rough that it lies even below $\lambda_9 = \lambda_{10}$ and prevents the method to obtain accurate results. The complementarity method exhibits the best results on rough meshes, but its accuracy on finer meshes is not competitive with the other methods due to its slow speed of convergences.

Further, we observe that the enclosure sizes of the lower eigenvalues are smaller than the enclosure sizes of the higher eigenvalues. All methods provide less accurate results as the index of the eigenvalue increases. This effect is highlighted in our results, because we present the absolute sizes of the enclosures. However, we would observe the loss of accuracy for the higher eigenvalues even if we plotted relative sizes of enclosures weighted by sizes of corresponding eigenvalues.

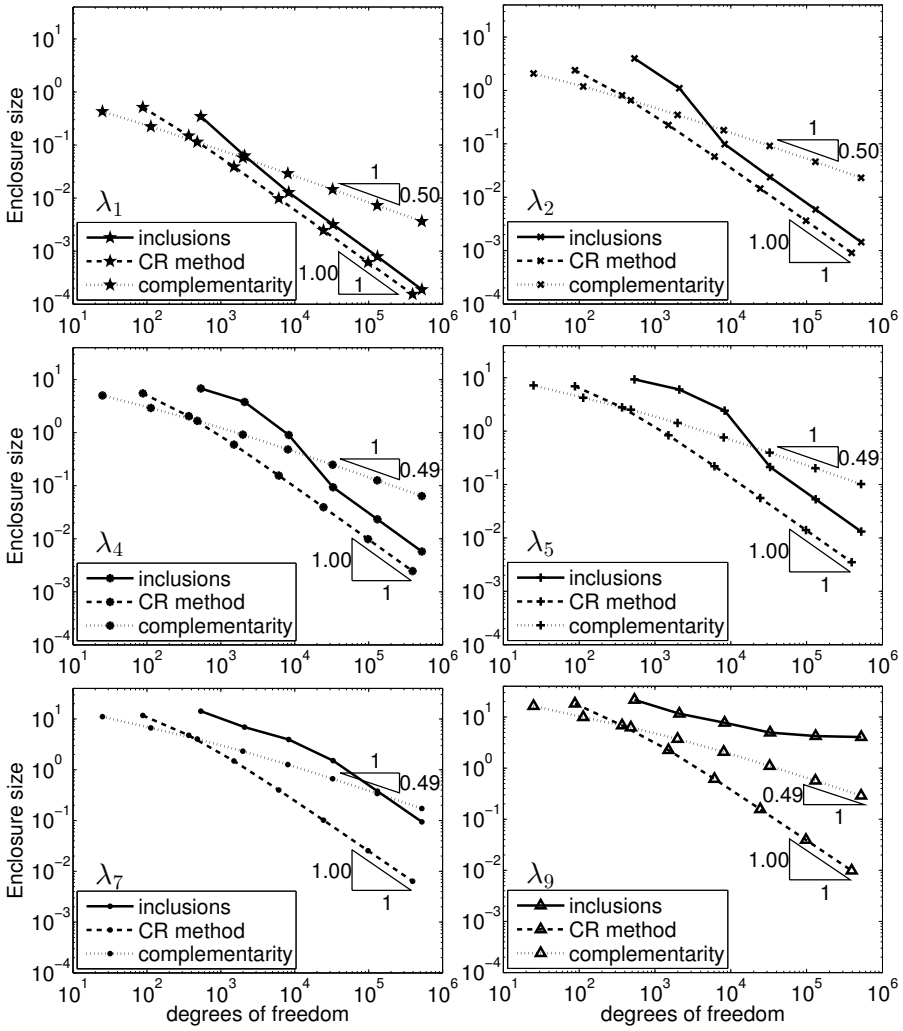

Figure 2: Convergence of enclosure sizes for the inclusions, CR, and complementary methods. The panels correspond to eigenvalues λ_1, λ_2, λ_4, λ_5, λ_7, and λ_9, respectively. The convergence curves for eigenvalues λ_3, λ_6, λ_8, and λ_{10} are very similar to the curves for λ_2, λ_5, λ_7, and λ_9, respectively, because these four eigenvalues are multiple with multiplicity two. The triangles indicate the experimental orders of convergence.

	a priori lower bound	the largest lower bound	the smallest upper bound
λ_1	1.197531	1.955284	1.955879
λ_2	1.790123	1.960219	1.960760
λ_3	2.777778	4.798073	4.801187
λ_4	4.160494	4.827345	4.830269
λ_5	4.197531	4.995027	4.996958
λ_6	4.790123	4.995043	4.996972
λ_7	5.777778	7.982102	7.987241
λ_8	5.938272	7.982176	7.987308
λ_9	7.160494	9.347872	9.358706
λ_{10}	8.111111	9.502020	9.512035

Table 2: The analytically computed *a priori* lower bounds, the largest computed lower bounds, and the smallest computed upper bounds on the first 10 eigenvalues for the dumbbell shaped domain.

6 Numerical results – a dumbbell shaped domain

In this section, we will apply the three methods described in Sections 2–4 to compute the lower and upper bounds on the first $m = 10$ eigenvalues of a problem proposed in [27]. It is the eigenvalue problem (1) posed in the dumbbell shaped domain $\Omega = (0,\pi)^2 \cup [\pi, 5\pi/4] \times (3\pi/8, 5\pi/8) \cup (5\pi/4, 9\pi/4) \times (0,\pi)$, see Figure 1 (right). This is a more realistic example, where the exact eigenvalues are not known.

The *a priori* lower bounds for the inclusions methods are obtained by enclosing the domain Ω into the rectangle $\widehat{\Omega} = (0, 9\pi/4) \times (0,\pi)$, where we can analytically find the eigenvalues. These *a priori* lower bounds together with the largest lower bounds and the smallest upper bounds computed are presented in Table 2. We observe that although the two-sided bounds are quite tight, the enclosing intervals overlap for λ_5 and λ_6 and for λ_7 and λ_8. On the chosen level of accuracy, we cannot decide whether these two pairs are multiple or isolated eigenvalues. On the other hand, λ_1 and λ_2 as well as λ_3 and λ_4 are tight pairs of eigenvalues and the computed two-sided bounds are sufficiently accurate to show that they are all isolated.

We use the same methodology as in the previous section and compare the three methods. The initial triangulation is depicted in Figure 1 (right). Figures 3–4 present the sizes of the eigenvalue enclosures for eigenvalues λ_1, λ_2, …, λ_{10} and their dependence on the number of degrees freedom. We recall that the number of degrees of freedom corresponds to $N^{\mathrm{mix}} = \dim \boldsymbol{W}_h + \dim Q_h$ for the inclusions method, to $N^{\mathrm{CR}} = \dim V_h^{\mathrm{CR}}$ for the CR method, and to $N^{\mathrm{conf}} = \dim V_h$ for the complementarity method.

We again observe that the CR method provides the most accurate results with respect to the needed number of degrees of freedom. The convergence rates

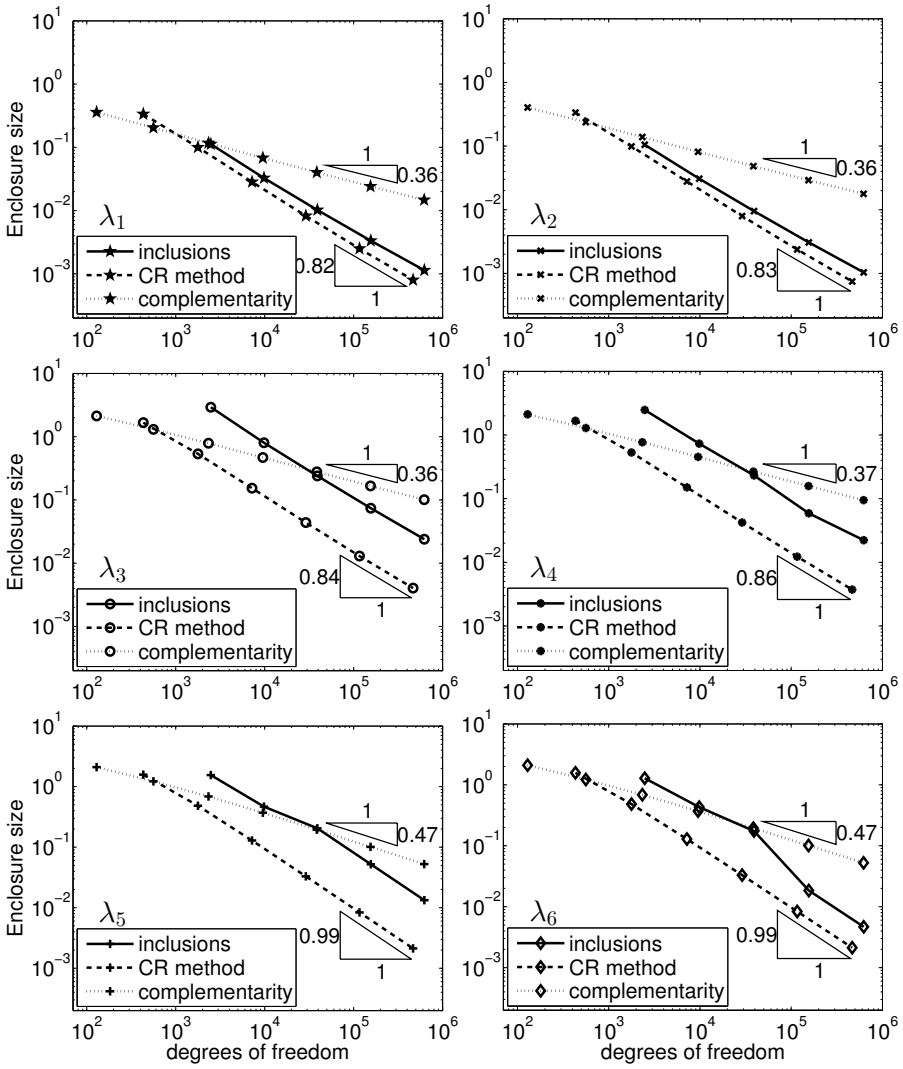

Figure 3: Enclosure sizes obtained by the inclusions, CR, and complementarity methods for eigenvalues λ_1, λ_2, ..., λ_6 on the dumbbell shaped domain. The triangles indicate the experimental orders of convergence.

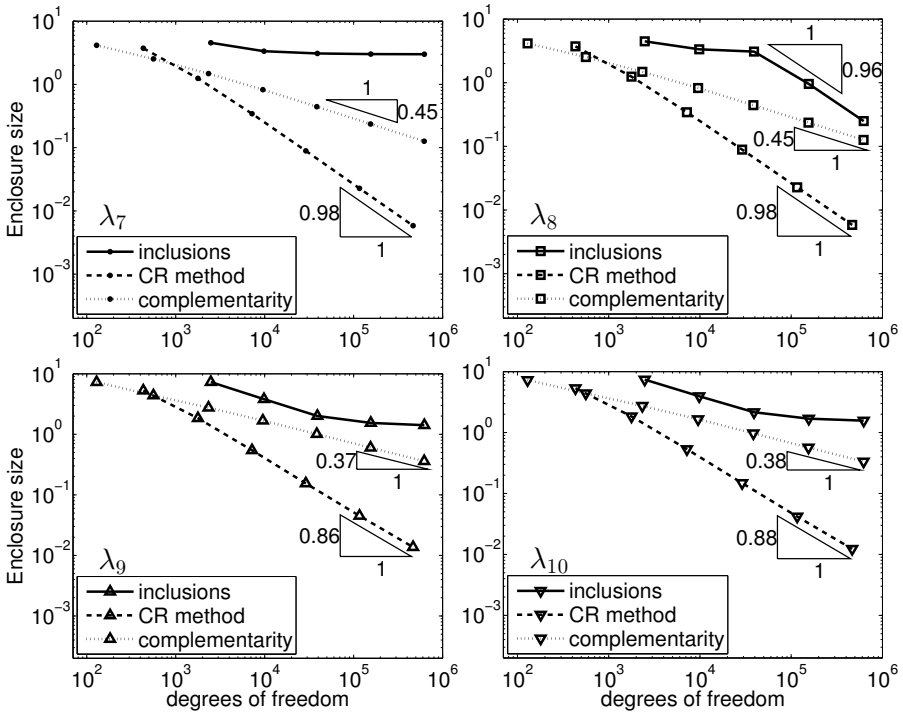

Figure 4: Enclosure sizes obtained by the inclusions, CR, and complementarity methods for eigenvalues λ_7, λ_8, ..., λ_{10} on the dumbbell shaped domain. The triangles indicate the experimental orders of convergence.

are in several cases spoiled by the singularities of eigenvectors at the reentrant corners of the domain. The optimal rates could be achieved by the adaptive mesh refinement, but this is not the goal of this paper. In any case, we clearly observe that the speed of convergence of the complementarity method is roughly half of the speed of the other two methods. On the other hand, the complementarity method provides the best results on the roughest meshes. As in the previous example, the inclusions method yields only slightly less accurate results than the CR method for the smallest eigenvalues. However, for larger eigenvalues its accuracy deteriorates and for λ_7, λ_9, and λ_{10} it even fails to converge. This is probably caused by too rough *a priori* lower bounds of the exact eigenvalues. In accordance with the previous example we also observe that the absolute sizes of eigenvalue enclosures increase for higher eigenvalues for all three methods.

7 Conclusions

We computed two-sided bounds of the first ten eigenvalues of the Dirichlet Laplacian for two numerical examples. For this purpose, we employed the inclusion, the CR, and the complementarity method on a series of uniformly refined meshes and compared the results.

The most accurate lower bounds with respect to the chosen numbers of degrees of freedom were obtained for the CR method. This fact can be expected, because the CR method is tailored specifically to the solved Laplace eigenvalue problem with Dirichlet boundary conditions. This makes the method the most specialized and least general out of the three compared methods. Moreover, it is not clear how the CR method could be generalized to problems with Neumann and mixed boundary conditions, to problems with variable coefficients, or to different types of eigenvalue problems such as the Steklov eigenvalue problem. Another slight disadvantage is the fact that dimension of V_h^{CR} is still larger than the dimension of V_h, which is used as a base space for the other two methods. On the other hand, the distinctive feature the CR method is that it does not require any *a pripori* information about the exact eigenvalues. It provides guaranteed lower bounds even on rough meshes and it takes into the account also the error caused by the matrix eigenvalue solver. However, here the method requires a closeness assumption that cannot be verified unless the exact eigenvalues of the matrix eigenvalue problem are known. In any case, the CR method is very promising and investigation of its possible generalizations seems to be very desirable.

The inclusions method lags only closely behind the CR method in terms of the accuracy especially for the smallest eigenvalues. The disadvantage of the inclusion method is the solution of the large mixed finite element problem (6)–(7). If the fluxes $\boldsymbol{\sigma}_{h,i}$ were computed locally and efficiently as in the complementarity method than the convergence curves of the inclusions method would be shifted considerably to the left, see Figures 2, 3 and 4, and the method would easily outperform the CR method. The other serious disadvantage of the method is

the need of the *a priori* lower bounds on eigenvalues. As we saw especially in the case of the larger eigenvalues, its accuracy strongly depends on the quality of these *a priori* lower bounds. In [6], the authors propose to use the homotopy method to obtain these *a priori* lower bounds. The homotopy method, however, seems to be difficult to automatize in the context of the finite element method. On the other hand, the advantage of the inclusions method is its generality and the fact that it is well developed in the literature. It can be generalized even to indefinite problems and to problems with essential spectrum. For example, its variant was used in [4] to find eigenvalue enclosures for the Maxwell eigenvalue problem.

The complementarity method provides the best results on rough meshes. However, its accuracy on finer meshes is not competitive due to its slow speed of convergence. It also requires an *a priori* information about the exact eigenvalues, but it is in the form of the relative closeness assumption (18). Since the standard finite element approximations $\Lambda_{h,i}$ given by (4) converge to λ_i, its is clear that this assumption will eventually be satisfied on a sufficiently fine mesh. In addition, if the computed lower bounds are sufficiently accurate then they can be used to verify the validity of the relative closeness assumption. The complementarity method is quite general and it can be applied to symmetric elliptic problems with mixed boundary conditions, variable coefficients, and various types of eigenvalue problems. It requires a flux reconstruction by solving small mixed finite element problems on patches of elements. Their solution takes certain computation time, but these problems are independent and can be easily solved in parallel. If the suboptimal rate of convergence is improved and the current research indicates that it is possible [9], then the complementarity method will be as competitive as the other two methods even in terms of accuracy.

An interesting question is whether the computed lower bounds are really below the exact eigenvalues. Let us first consider the hypothetical case of exact arithmetic. The inclusion method provides guaranteed lower bounds even if the corresponding matrix problem is not solved exactly, because the approximation $\tilde{u}_i$ and $\tilde{\boldsymbol{\sigma}}_i$ in Theorem 1 can be arbitrary. However, the crucial requirement is the knowledge of the *a priori* lower bounds. The CR method provides guaranteed lower bounds (10) if the matrix eigenvalue problem (11) is solved exactly. However, even in the case of the exact arithmetic the iterative matrix algorithms produce iteration errors and the practical lower bound (12) should be employed. The bound (12) is valid if the computed eigenvalue $\tilde{\lambda}_i^{\mathrm{CR}}$ is closer to the exact discrete eigenvalue λ_i^{CR} than to any other discrete eigenvalue. This assumption is difficult to verify, because the exact discrete eigenvalues are inaccessible. The guaranteed knowledge of its validity is an *a priori* information, which is in a sense of the same kind as the *a priori* information required by the other two methods. The complementarity method provides guaranteed lower bounds in a similar spirit as the other two methods. Numerical inaccuracies in the flux reconstruction $\boldsymbol{q}_{h,i}$ are irrelevant, because any flux reconstruction lying in $\boldsymbol{H}(\mathrm{div}, \Omega)$ yields guaranteed lower bounds. The only relevant condition is the validity of the relative closeness assumption (18). However, it is guaranteed

only if an *a priori* knowledge about the exact eigenvalues is available.

Thus, to conclude, all these methods require an *a priori* information about the spectrum in order to guarantee the lower bounds even in the hypothetical case of the exact arithmetic. To overcome the problem of round-off errors in the floating-point arithmetic, it is proposed, for example in [5] and [6], to verify the computed bounds by using the interval arithmetic. In any case, the performed numerical experiments indicate that all the methods are quite robust in providing lower bounds on exact eigenvalues. For example, we used the known exact eigenvalues and verified that all methods really produced lower bounds on the exact eigenvalues in all computed cases.

To conclude, we are convinced that two-sided bounds of eigenvalues are highly relevant to compute, because they enable reliable control of the accuracy of the computed approximations. We believe that the presented methods are of practical value, because they are applicable in the context of the standard finite element method. We also believe that the presented results enable practitioners to choose the most suitable method for their purposes. Finally, we believe that these results encourage them to compute both upper and lower bounds on eigenvalues, because these enable full control of the accuracy and yield highly reliable numerical results.

References

[1] Andreev, A. and Racheva, M.: Two-sided bounds of eigenvalues of second- and fourth-order elliptic operators. Appl. Math. **59** (2014), 371–390.

[2] Armentano, M.G. and Durán, R.G.: Asymptotic lower bounds for eigenvalues by nonconforming finite element methods. Electron. Trans. Numer. Anal. **17** (2004), 93–101 (electronic).

[3] Babuška, I. and Osborn, J.E.: Eigenvalue problems. In: *Handbook of numerical analysis, Vol. II*, pp. 641–787. Handb. Numer. Anal., II, North-Holland, Amsterdam, 1991.

[4] Barrenechea, G.R., Boulton, L., and Boussaïd, N.: Finite element eigenvalue enclosures for the Maxwell operator. SIAM J. Sci. Comput. **36** (2014), A2887–A2906. doi:10.1137/140957810. URL `http://dx.doi.org/10.1137/140957810`.

[5] Behnke, H. and Goerisch, F.: Inclusions for eigenvalues of selfadjoint problems. In: *Topics in validated computations (Oldenburg, 1993)*, *Stud. Comput. Math.*, vol. 5, pp. 277–322. North-Holland, Amsterdam, 1994. doi:10.1016/0021-8502(94)90369-7. URL `http://dx.doi.org/10.1016/0021-8502(94)90369-7`.

[6] Behnke, H., Mertins, U., Plum, M., and Wieners, C.: Eigenvalue inclusions via domain decomposition. Proc. R. Soc. Lond., Ser. A, Math. Phys. Eng. Sci. **456** (2000), 2717–2730. doi:10.1098/rspa.2000.0635.

[7] Boffi, D.: Finite element approximation of eigenvalue problems. Acta Numer. **19** (2010), 1–120. doi:10.1017/S0962492910000012. URL http://dx.doi.org/10.1017/S0962492910000012.

[8] Braess, D. and Schöberl, J.: Equilibrated residual error estimator for edge elements. Math. Comp. **77** (2008), 651–672. doi:10.1090/S0025-5718-07-02080-7. URL http://dx.doi.org/10.1090/S0025-5718-07-02080-7.

[9] Cancès, E., Dusson, G., Maday, Y., Stamm, B., and Vohralík, M.: Guaranteed and robust a posteriori bounds for laplace eigenvalues and eigenvectors: conforming approximations. preprint hal-01194364 (2015), 25p.

[10] Carstensen, C. and Merdon, C.: Computational survey on a posteriori error estimators for nonconforming finite element methods for the Poisson problem. J. Comput. Appl. Math. **249** (2013), 74–94. doi:10.1016/j.cam.2012.12.021. URL http://dx.doi.org/10.1016/j.cam.2012.12.021.

[11] Carstensen, C. and Gedicke, J.: Guaranteed lower bounds for eigenvalues. Math. Comp. **83** (2014), 2605–2629. doi:10.1090/S0025-5718-2014-02833-0. URL http://dx.doi.org/10.1090/S0025-5718-2014-02833-0.

[12] Harrell, E.M.: Generalizations of Temple's inequality. Proc. Amer. Math. Soc. **69** (1978), 271–276.

[13] Haslinger, J. and Hlaváček, I.: Convergence of a finite element method based on the dual variational formulation. Apl. Mat. **21** (1976), 43–65.

[14] Hlaváček, I.: Some equilibrium and mixed models in the finite element method. In: *Mathematical models and numerical methods (Papers, Fifth Semester, Stefan Banach Internat. Math. Center, Warsaw, 1975)*, *Banach Center Publ.*, vol. 3, pp. 147–165. PWN, Warsaw, 1978.

[15] Hlaváček, I. and Křížek, M.: Internal finite element approximations in the dual variational method for second order elliptic problems with curved boundaries. Apl. Mat. **29** (1984), 52–69.

[16] Hu, J., Huang, Y., and Lin, Q.: Lower bounds for eigenvalues of elliptic operators: by nonconforming finite element methods. J. Sci. Comput. **61** (2014), 196–221. doi:10.1007/s10915-014-9821-5. URL http://dx.doi.org/10.1007/s10915-014-9821-5.

[17] Hu, J., Huang, Y., and Shen, Q.: The lower/upper bound property of approximate eigenvalues by nonconforming finite element methods for elliptic operators. J. Sci. Comput. **58** (2014), 574–591. doi:10.1007/s10915-013-9744-6. URL http://dx.doi.org/10.1007/s10915-013-9744-6.

[18] Kato, T.: On the upper and lower bounds of eigenvalues. J. Phys. Soc. Japan **4** (1949), 334–339.

[19] Kuttler, J.R. and Sigillito, V.G.: Bounding eigenvalues of elliptic operators. SIAM J. Math. Anal. **9** (1978), 768–778.

[20] Lehmann, N.J.: Beiträge zur numerischen Lösung linearer Eigenwertprobleme. I. Z. Angew. Math. Mech. **29** (1949), 341–356.

[21] Lehmann, N.J.: Beiträge zur numerischen Lösung linearer Eigenwertprobleme. II. Z. Angew. Math. Mech. **30** (1950), 1–16.

[22] Luo, F., Lin, Q., and Xie, H.: Computing the lower and upper bounds of Laplace eigenvalue problem: by combining conforming and nonconforming finite element methods. Sci. China Math. **55** (2012), 1069–1082. doi:10.1007/s11425-012-4382-2. URL `http://dx.doi.org/10.1007/s11425-012-4382-2`.

[23] Plum, M.: Guaranteed numerical bounds for eigenvalues. In: *Spectral theory and computational methods of Sturm-Liouville problems (Knoxville, TN, 1996)*, *Lecture Notes in Pure and Appl. Math.*, vol. 191, pp. 313–332. Dekker, New York, 1997.

[24] Šebestová, I. and Vejchodský, T.: Two-sided bounds for eigenvalues of differential operators with applications to Friedrichs, Poincaré, trace, and similar constants. SIAM J. Numer. Anal. **52** (2014), 308–329. doi:10.1137/13091467X. URL `http://dx.doi.org/10.1137/13091467X`.

[25] Šebestová, I. and Vejchodský, T.: Two-sided bounds of eigenvalues – local efficiency and convergence of adaptive algorithm. preprint arXiv (2016), 28p.

[26] Temple, G.: The theory of Rayleigh's principle as applied to continuous systems. Proc. Roy. Soc. London Ser. A **119** (1928), 276–293.

[27] Trefethen, L.N. and Betcke, T.: Computed eigenmodes of planar regions. In: *Recent advances in differential equations and mathematical physics*, *Contemp. Math.*, vol. 412, pp. 297–314. Amer. Math. Soc., Providence, RI, 2006. doi:10.1090/conm/412/07783. URL `http://dx.doi.org/10.1090/conm/412/07783`.

[28] Vejchodský, T.: Complementarity based a posteriori error estimates and their properties. Math. Comput. Simulation **82** (2012), 2033–2046. doi:http://dx.doi.org/10.1016/j.matcom.2011.06.001.

[29] Vejchodský, T.: Complementary error bounds for elliptic systems and applications. Appl. Math. Comput. **219** (2013), 7194–7205.

[30] Yang, Y., Han, J., Bi, H., and Yu, Y.: The lower/upper bound property of the Crouzeix-Raviart element eigenvalues on adaptive meshes. J. Sci. Comput. **62** (2015), 284–299. doi:10.1007/s10915-014-9855-8. URL `http://dx.doi.org/10.1007/s10915-014-9855-8`.